Production cross sections of ^{169}Yb by the proton-induced reaction on ^{169}Tm

Moemi Saito[a], Masayuki Aikawa[a,b,*], Tomohiro Murata[a], Yukiko Komori[c], Hiromitsu Haba[c],
Sándor Takács[d], Ferenc Ditrói[d], Zoltán Szűcs[d]

[a] *Graduate School of Biomedical Science and Engineering, Hokkaido University, Sapporo 060-8638, Japan*

[b] *Faculty of Science, Hokkaido University, Sapporo 060-0810, Japan*

[c] *Nishina Center for Accelerator-Based Science, RIKEN, Wako 351-0198, Japan*

[d] *Institute for Nuclear Research (ATOMKI), 4026 Debrecen, Hungary*

Abstract

Activation cross sections of the ^{169}Tm(p,n)^{169}Yb reaction were measured up to 18 MeV. The stacked-foil activation technique and the high-resolution gamma-ray spectrometry were adopted to derive the cross sections. The result is compared with previous experimental data and theoretical model calculation. Physical yield of ^{169}Yb is derived from the measured cross sections and compared with those from other production routes.

Keyword

Ytterbium-169; Proton irradiation; Thulium target; Cross section; Excitation function

1. Introduction

Ytterbium-169 ($T_{1/2}$ = 32.018 d) is a therapeutic radioisotope. It decays with emissions of Auger electrons, X-rays and low energy gamma-rays. These decay properties of ^{169}Yb are appropriate for brachytherapy [1]. For practical use, the best process should be selected for its production among all possible reactions. One of them is the neutron capture reaction on the stable ytterbium isotope ^{168}Yb, of which the natural isotopic ratio is only 0.123%. Therefore, enriched ^{168}Yb target material is required for this production process. Another possibility to produce ^{169}Yb is the use of charged-particle-induced reactions. Proton, deuteron and alpha particles can be considered. We have decided to investigate systematically the production of ^{169}Yb via charged-particle-induced reactions. The reactions by deuteron- [2] and alpha-particle-induced reactions on ^{169}Tm, and the alpha-particle on ^{nat}Er [3] have already been studied. In this work, as a part of this systematic investigation of the ^{169}Yb production, we focused on the proton-induced reaction on ^{169}Tm.

^{169}Yb can be formed in the (p,n) reaction on the monoisotopic element ^{169}Tm. Results of three previous studies for the ^{169}Tm(p,n)^{169}Yb reaction [4–6] are available in the EXFOR library [7]. However, there is a large discrepancy among the available experimental data. To solve this problem, we have investigated the excitation function of the ^{169}Tm(p,n)^{169}Yb reaction up to 18 MeV. The resulted cross sections are presented in this paper. The expected physical yield of ^{169}Yb is also derived from the measured cross sections. The

* Corresponding author: Masayuki AIKAWA, aikawa@sci.hokudai.ac.jp

calculated yield is compared with those of the possible deuteron- and alpha-particle-induced reactions. Production of ^{167,168}Tm, as potential side products, was also investigated.

2. Experimental

The activation cross sections of the proton-induced reactions on ^{169}Tm were measured. The experiment was performed using the MGC-20E cyclotron at Institute for Nuclear Research (ATOMKI), Hungary. To derive the activation cross sections, well-established methods, the stacked-foil activation technique and the high-resolution gamma-ray spectrometry were adopted.

The target consisted of thin metallic foils of ^{169}Tm (99.0% purity, Goodfellow Co., Ltd., UK) and ^{nat}Ti (99.6% purity, Nilaco Corp., Japan). The ^{nat}Ti foils were interleaved for degradation of the beam energy and for assessment of beam parameters and target thicknesses. The original sizes and weights of the Tm and Ti foils were measured for the average thicknesses before cutting them up. The average thicknesses of the Tm and Ti foils were found to be 21.0 and 9.1 mg/cm^2, respectively. The foils were cut into small pieces of 6 × 6 mm to fit a target holder. Sixteen sets of Tm-Ti-Ti foils were stacked into the target holder. The first Ti foil in each set served as a catcher foil of the recoiled products from the previous Tm foil. The second Ti foil of each set was used to monitor the beam parameters because its activity loss was considered to be compensated by the reaction products recoiled from the first Ti foil.

The assembled target was irradiated for 30 min with an 18-MeV proton beam. The average beam intensity was 210 nA measured by a Faraday cup. Energy degradation in the target was calculated using stopping powers obtained from the SRIM code [8]. As the ^{169}Tm is a monoisotopic element and the ^{168,170}Yb isotopes are stable, no ytterbium radio-contamination is expected at the used bombarding proton energy. The possible high specific activity of ^{169}Yb without the contamination is advantageous for practical use in medicine.

Gamma-rays emitted from the irradiated foils were measured by an HPGe detector (Canberra) without chemical separation. Each foil was measured three times after a cooling time of 1.8-134 days. The deadtime during the measurements was kept below ~2%. The gamma-ray spectra were recorded by the software Genie-2000 (Canberra) and analyzed by Gamma Studio (SEIKO EG&G). Nuclear data required for deduction of cross sections were obtained from NuDat 2.8 [9], LiveChart [10] and QCalc [11]. The decay data used in the data analysis are summarized in Table 1.

The ^{nat}Ti(p,x)^{48}V monitor reaction was used to assess the beam parameters and to check the target thicknesses. The cross sections of the monitor reaction were derived from the gamma-line at 983.53 keV (I_γ = 99.98%) emitted with the decay of ^{48}V ($T_{1/2}$ = 15.97 d) in every second Ti foil. The result was compared with the two sets of the IAEA recommended values [12,13] in Fig. 1. The shape of our result is more consistent with the older recommended data set [13]. The primary beam energy, which was initially derived from the settings of the cyclotron parameters, was adjusted to 17.6 MeV. The average beam intensity, measured on the Faraday cup like target holder without suppressor voltage, had to be reduced by 10% to 189 nA due to the effect of secondary electrons. With the modified beam parameters and the originally determined

average target thicknesses the cross section points of the monitor reaction were in perfect agreement with the earlier recommended data [13] indicating a proper energy loss calculation throughout the whole layered target. In the data analysis the modified beam parameters and the originally determined foil thicknesses were adopted.

Table 1. Reaction and decay data for ^{169}Yb production

Nuclide	Half-life	Decay mode (%)	E_γ (keV)	I_γ (%)	Contributing reaction	Q-value (MeV)
^{169g}Yb	32.02 d	ε (100)	63.12	43.62(23)	^{169}Tm(p,n)	-1.7
			177.21	**22.28(11)**		
			197.96	35.93(12)		
^{168}Tm	93.1 d	β^- (0.01)	184.30	18.15(16)	^{169}Tm(p,d)	-5.8
		ε+β^+ (99.99)	198.25	54.49(16)	^{169}Tm(p,pn)	-8.0
			447.52	23.98(11)		
			815.99	**50.95(16)**		
^{167}Tm	9.25 d	ε (100)	**207.80**	**42(8)**	^{169}Tm(p,t)	-6.4
					^{169}Tm(p,dn)	-12.6
					^{169}Tm(p,p2n)	-14.9
					^{169}Tm(p,3n)^{167}Yb(ε)	-17.6
^{48}V	15.97 d	ε+β^+ (100)	**983.53**	**99.98(4)**	^{nat}Ti(p,x)	

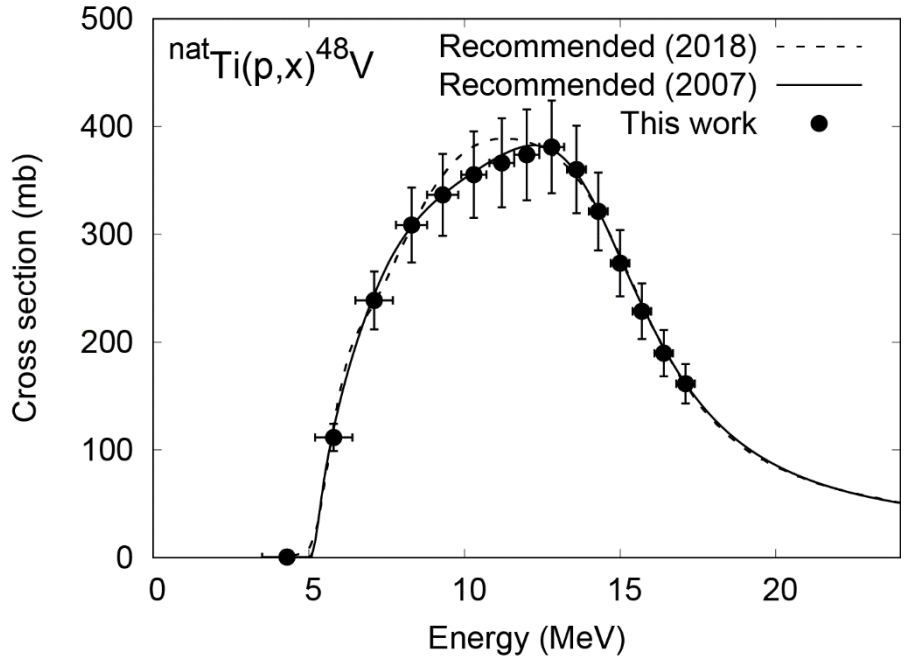

Fig. 1. Excitation function of the ^{nat}Ti(p,x)^{48}V monitor reaction compared with the recommended values [12,13].

3. Results and discussion

The activation cross sections of the proton-induced reactions on ^{169}Tm for production of ^{169}Yb and co-produced radionuclides, ^{167,168}Tm, were determined up to 17.6 MeV. ^{166}Tm could not be measured although the threshold energy of its production reaction is 15.2 MeV. The cross sections are numerically presented in Table 2 and graphically shown in Figs. 2-4. The results are compared with the experimental data published earlier [4–6] and the result of theoretical model calculation in the TENDL-2019 library [14]. Physical yield of ^{169}Yb is deduced from the cross sections obtained in this work and shown in Fig. 5.

The estimated total uncertainty of the cross sections was 11.3-47.0% calculated as the square root of the quadratic summation of each component. The considered propagating error sources are statistical uncertainty (0.6-7.6%, except 17.7-41.5% for ^{167}Tm), target thickness (1%), target purity (1%), beam intensity (10%), detector efficiency (5%) and gamma-intensity (0.3-19.0%).

The uncertainty of the energy scale includes the initial uncertainty of the beam ±0.2 MeV and uncertainty from the energy loss calculation and straggling effect. The cumulative uncertainty in the last target foils reached ±0.8 MeV.

Table 2. Measured cross sections

Energy (MeV)	^{169}Tm(p,n)^{169}Yb (mb)	^{169}Tm(p,x)^{168}Tm (mb)	^{169}Tm(p,x)^{167}Tm (mb)
17.5 ±0.3	30.7 ±3.8	19.9 ±2.2	2.05 ±0.58
16.8 ±0.3	41.7 ±5.0	16.8 ±1.9	1.47 ±0.51
16.2 ±0.4	44.5 ±5.4	11.3 ±1.3	1.23 ±0.58
15.5 ±0.4	51.1 ±6.1	6.97 ±0.79	
14.8 ±0.4	63.8 ±7.6	4.02 ±0.45	
14.1 ±0.4	71.4 ±8.1	1.68 ±0.19	
13.3 ±0.4	95.1 ±11.0	0.665 ±0.079	
12.5 ±0.4	126 ±14	0.175 ±0.024	
11.7 ±0.5	127 ±15		
10.8 ±0.5	159 ±18		
9.9 ±0.5	160 ±18		
8.9 ±0.5	127 ±15		
7.9 ±0.6	65.4 ±7.6		
6.7 ±0.7	16.4 ±2.0		
5.3 ±0.8	1.56 ±0.18		

3.1 The ^{169}Tm(p,n)^{169}Yb reaction

In the analysis the 177.21-keV gamma-rays (I_γ = 22.28%) emitted with the ^{169}Yb decay ($T_{1/2}$ = 32.018 d) were used. The other strong gamma-rays at 63.12 (I_γ = 43.62%) and 197.96 keV (I_γ = 35.93%) were unselected to avoid possible interference with X-rays and the 198.25-keV gamma-rays from the ^{168}Tm decay. The cross sections of the ^{169}Tm(p,n)^{169}Yb reaction were derived from the measurements after an average cooling time of 4.5 days. The result is shown in Fig. 2 in comparison with the previous experimental data [4–6] and the TENDL-2019 data [14]. The peak amplitude of the data of Birattari et al. (1973) [4] is consistent with our result. However, the data of Spahn et al. (2005) [5] are more scattered and show two times larger amplitude and larger uncertainties than ours, which may be explained by the used thulium(III) oxide (Tm_2O_3) target material and the sedimentation target preparation method. With the data of Tarkanyi et al. (2012) [6] only an acceptable agreement of tendency can be confirmed at higher energy, as their data points are above the 24-MeV proton energy. The peak of the TENDL-2019 data show the similar amplitude with ours, however its shape is different. The width of the curve is narrower and the maximum energy position is lower than ours.

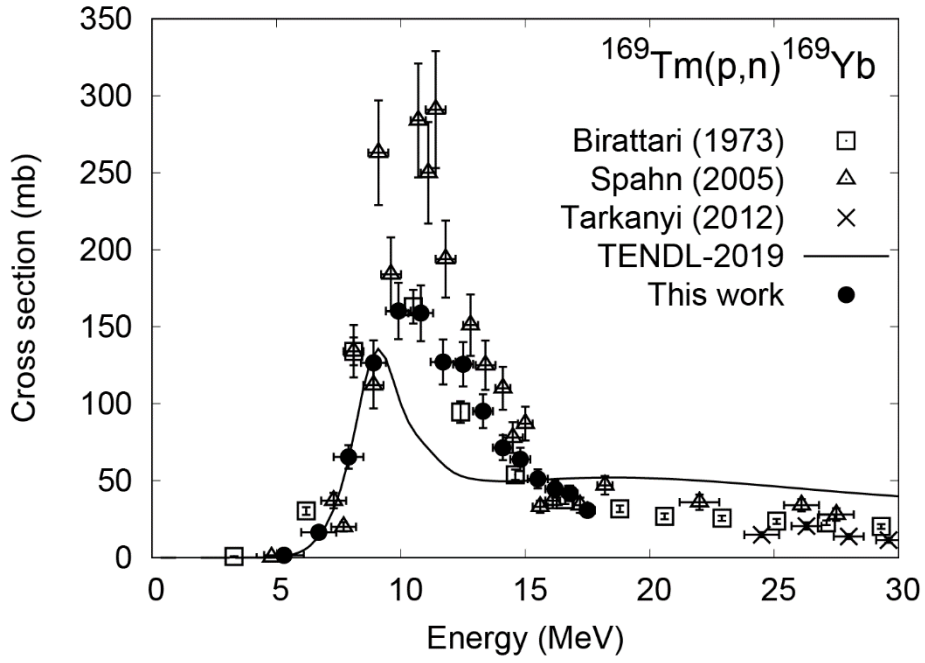

Fig. 2. Excitation function of the ^{169}Tm(p,n)^{169}Yb reaction with the previous data [4–6] and the TENDL-2019 data [14].

3.2 The ^{169}Tm(p,x)^{168}Tm reaction

The cross sections of the ^{169}Tm(p,x)^{168}Tm reaction was determined from the measurements using the gamma-rays of 815.99 keV (I_γ = 50.95%) from the decay of ^{168}Tm ($T_{1/2}$ = 93.1 d). The more intense gamma-ray at 198.25 keV (I_γ = 54.49%) was unselected to avoid the interference with the 197.96-keV gamma-rays from the ^{169}Tm decay. Our result with the previous experimental data [6] and the TENDL-2019 data [14] is shown in Fig. 3. The energy region of the previous data is higher than the particle energy in this experiment, therefore the data points are not overlapped, but follow the tendency predicted by the TENDL-2019 calculation. However, the TENDL-2019 data underestimate our cross sections at low energies.

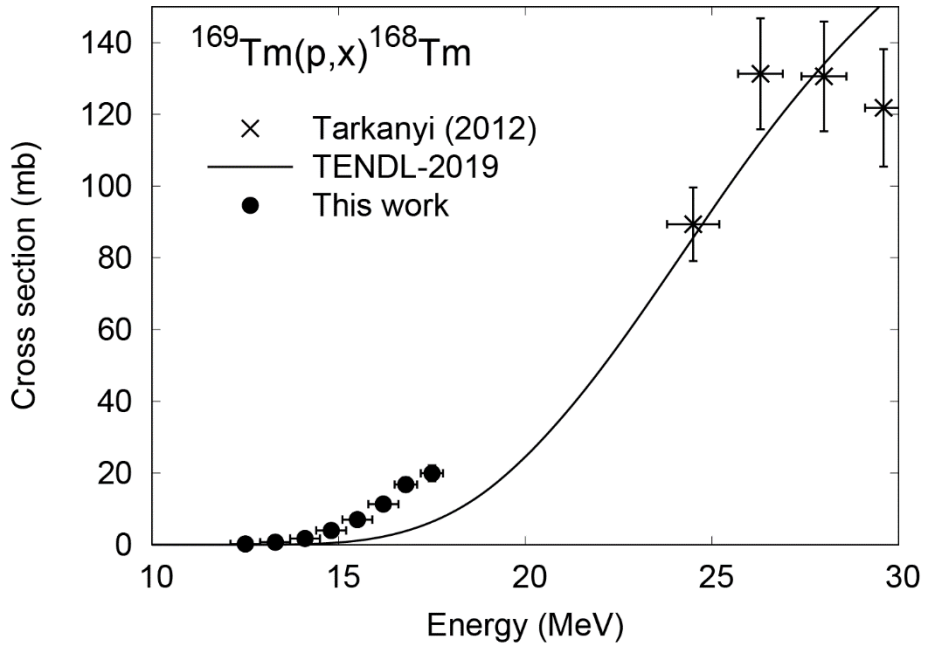

Fig. 3. Cross sections of the ^{169}Tm(p,x)^{168}Tm reaction with the previous data [6] and the TENDL-2019 data [14].

3.3 The ^{169}Tm(p,x)^{167}Tm reaction

^{167}Tm can be formed in the (p,t), (p,dn) and (p,p2n) direct reactions and above 17.7 MeV also indirectly by the decay of ^{167}Yb. The gamma-rays at 207.80 keV (I_γ = 42%) emitted with the decay of ^{167}Tm ($T_{1/2}$ = 9.25 d) were assessed for the irradiated foils. As the threshold energy of the ^{169}Tm(p,3n)^{167}Yb reaction is 17.7 MeV a negligibly small contribution from the decay of ^{167}Yb ($T_{1/2}$ = 17.5 min) can be expected only in the first foil. The deduced cross sections of the ^{169}Tm(p,x)^{167}Tm reaction in this energy region is small and due to the large uncertainty of the gamma-intensity data (19%) and low statistics of the photo-peak (17.7-41.5%), the total uncertainty becomes large (28.3-47.0%).

The result is shown in Fig. 4 with the cumulative cross sections of the earlier study [6] and the TENDL-2019 library [14]. The contribution from the decay of ^{167}Yb at the higher energy region is much higher than the direct production of ^{167}Tm.

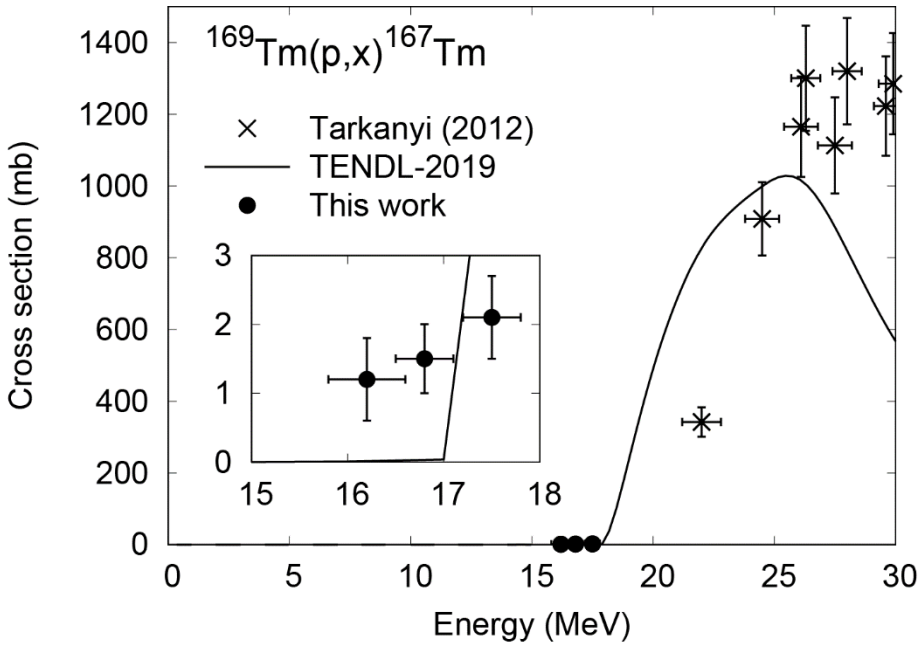

Fig. 4. Excitation function of the ^{169}Tm(p,x)^{167}Tm reaction with the previous data [6] and the TENDL-2019 data [14].

3.4 Physical yield of ^{169}Yb

Physical yield of ^{169}Yb in the ^{169}Tm(p,n)^{169}Tm reaction was derived from the cross sections measured in this work. The result is shown in Fig. 5 in comparison with the yields derived from the experimental cross sections of the ^{169}Tm(d,2n)^{169}Yb [2] and ^{nat}Er(α,x)^{169}Yb reactions [3] measured previously by us. One can conclude that a general PET proton cyclotron having an energy of around 18 MeV can be used to produce ^{169}Yb. However, cyclotrons with the deuteron option are more preferable to produce ^{169}Yb. Using chemical separation, one can obtain ^{169}Yb without any radioactive impurities because the co-produced ^{168}Yb and ^{170}Yb are stable.

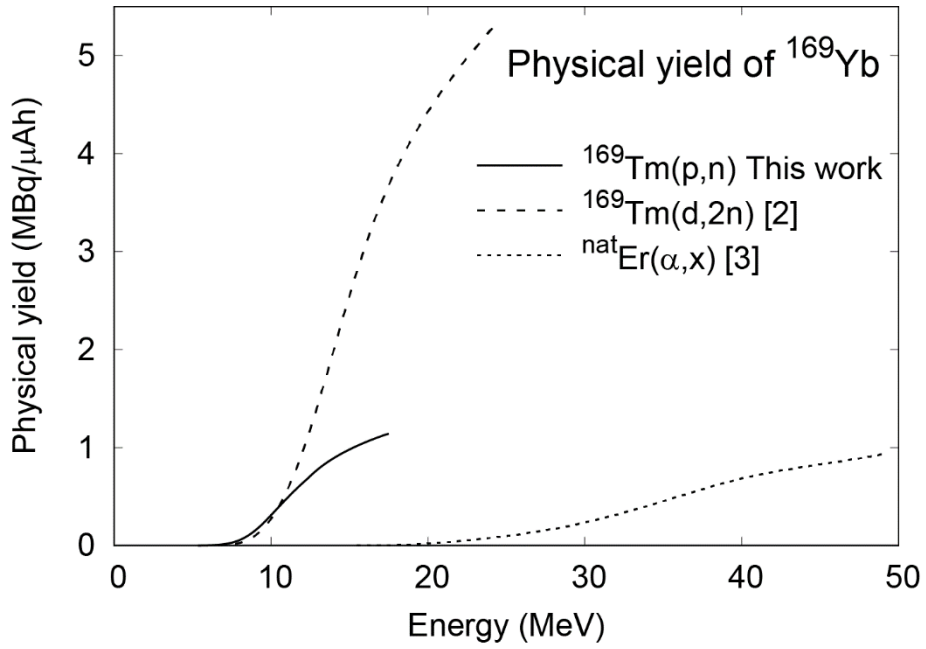

Fig. 5. Physical yields of ^{169}Yb deduced from the measured cross sections in this work and previous studies on the ^{169}Tm(d,2n)^{169}Yb [2] and ^{nat}Er(α,x)^{169}Yb reactions [3].

4. Summary

Activation cross sections were measured for proton-induced reactions on ^{169}Tm up to 18 MeV. The experiment was performed using the cyclotron at ATOMKI. The well-established methods, the stacked-foil activation technique and the high-resolution gamma-ray spectrometry, were adopted. The measured production cross sections of ^{169}Yb and ^{167,168}Tm were compared with previous experimental data and theoretical model calculation and general agreements were found. The physical yield was derived from the ^{169}Tm(p,n)^{169}Yb reaction and compared with those of the ^{169}Tm(d,2n)^{169}Yb and ^{nat}Er(α,x)^{169}Yb reactions. The ^{169}Tm(p,n)^{169}Yb reaction can provide ^{169}Yb. The comparison also indicates that the deuteron-induced reaction on ^{169}Tm can provide the higher yield of ^{169}Yb than the other production routes.

Acknowledgement

This work was carried out at Institute for Nuclear Research (ATOMKI), Hungary. This work was partly supported by "Optimization of accelerator production routes of the new theranostic radioisotopes Sc-47 and Cu-67 (FY2019-2020 and NKM-43/2019)", under the Japan - Hungary Research Cooperative Program, JSPS and HAS. The work is also supported by JSPS KAKENHI Grant Number 17K07004.

Declarations of interest

None

Reference

[1] K.L. Leonard, T.A. DiPetrillo, J.J. Munro, D.E. Wazer, A novel ytterbium-169 brachytherapy source and delivery system for use in conjunction with minimally invasive wedge resection of early-stage lung cancer, Brachytherapy. 10 (2011) 163–169. doi:10.1016/j.brachy.2010.06.006.

[2] M. Saito, M. Aikawa, Y. Komori, H. Haba, S. Takács, Production cross sections of ^{169}Yb and Tm isotopes in deuteron-induced reactions on ^{169}Tm, Appl. Radiat. Isot. 125 (2017) 23–26. doi:10.1016/j.apradiso.2017.04.010.

[3] M. Saito, M. Aikawa, M. Sakaguchi, N. Ukon, Y. Komori, H. Haba, Production cross sections of ytterbium and thulium radioisotopes in alpha-induced nuclear reactions on natural erbium, Appl. Radiat. Isot. 154 (2019) 108874. doi:10.1016/j.apradiso.2019.108874.

[4] C. Birattari, E. Gadioli, E. Gadioli Erba, A.M. Grassi Strini, G. Strini, G. Tagliaferri, PRE-EQUILIBRIUM PROCESSES IN (p,n) REACTIONS, Nucl. Phys. A. 201 (1973) 579–592.

[5] I. Spahn, S. Takács, Y.N. Shubin, F. Tárkányi, H.H. Coenen, S.M. Qaim, Cross-section measurement of the ^{169}Tm(p,n) reaction for the production of the therapeutic radionuclide ^{169}Yb and comparison with its reactor-based generation, Appl. Radiat. Isot. 63 (2005) 235–239.

[6] F. Tárkányi, A. Hermanne, S. Takács, F. Ditrói, I. Spahn, A. V. Ignatyuk, Activation cross-sections of proton induced nuclear reactions on thulium in the 20-45MeV energy range, Appl. Radiat. Isot. 70 (2012) 309–314. doi:10.1016/j.apradiso.2011.08.020.

[7] N. Otuka, E. Dupont, V. Semkova, B. Pritychenko, A.I. Blokhin, M. Aikawa, S. Babykina, M. Bossant, G. Chen, S. Dunaeva, R.A. Forrest, T. Fukahori, N. Furutachi, S. Ganesan, Z. Ge, O.O. Gritzay, M. Herman, S. Hlavač, K. Kato, B. Lalremruata, Y.O. Lee, A. Makinaga, K. Matsumoto, M. Mikhaylyukova, G. Pikulina, V.G. Pronyaev, A. Saxena, O. Schwerer, S.P. Simakov, N. Soppera, R. Suzuki, S. Takács, X. Tao, S. Taova, F. Tárkányi, V. V. Varlamov, J. Wang, S.C. Yang, V. Zerkin, Y. Zhuang, Towards a More complete and accurate experimental nuclear reaction data library (EXFOR): International collaboration between nuclear reaction data centres (NRDC), Nucl. Data Sheets. 120 (2014) 272–276. doi:10.1016/j.nds.2014.07.065.

[8] J.F. Ziegler, J.P. Biersack, M.D. Ziegler, SRIM: the Stopping and Range of Ions in Matter, (2008). http://www.srim.org.

[9] National Nuclear Data Center, Nuclear structure and decay data on-line library, Nudat 2.8, (2019). http://www.nndc.bnl.gov/nudat2/.

[10] International Atomic Energy Agency, LiveChart of Nuclides, (2009). https://www-nds.iaea.org/livechart/.

[11] B. Pritychenko, A. Sonzogni, Q-value Calculator (QCalc), (2003). http://www.nndc.bnl.gov/qcalc/.

[12] A. Hermanne, A. V. Ignatyuk, R. Capote, B. V. Carlson, J.W. Engle, M.A. Kellett, T. Kibédi, G. Kim, F.G. Kondev, M. Hussain, O. Lebeda, A. Luca, Y. Nagai, H. Naik, A.L. Nichols, F.M. Nortier, S. V. Suryanarayana, S. Takács, F.T. Tárkányi, M. Verpelli, Reference Cross Sections for Charged-particle Monitor Reactions, Nucl. Data Sheets. 148 (2018) 338–382. doi:10.1016/j.nds.2018.02.009.

[13] F. Tárkányi, S. Takács, K. Gul, A. Hermanne, M.G. Mustafa, M. Nortier, P. Obložinský, S.M. Qaim, B. Scholten, Y.N. Shubin, Z. Yousiang, Beam monitor reactions, in: Charg. Part. Cross-Section Database Med. Radioisot. Prod. IAEA-TECDOC-1211, 2001.

[14] A.J. Koning, D. Rochman, J.-C. Sublet, N. Dzysiuk, M. Fleming, S. van der Marck, TENDL: Complete Nuclear Data Library for Innovative Nuclear Science and Technology, Nucl. Data Sheets. 155 (2019) 1–55. doi:10.1016/j.nds.2019.01.002.